

# Probing metastable Sm2+ and optically stimulated tunnelling emission in YPO4: Ce, Sm

**Prasad, Amit Kumar; Kook, Myung Ho; Jain, Mayank**

*Published in:*
Radiation Measurements

*Link to article, DOI:*
10.1016/j.radmeas.2016.11.012

*Publication date:*
2017

*Document Version*
Peer reviewed version

# Probing Metastable $Sm^{2+}$ and Optically Stimulated Tunnelling Emission in $YPO_4$: Sm, Ce

A. K. Prasad*, M. Kook, M. Jain

*Center for Nuclear Technologies, Technical University of Denmark, DTU Risø Campus, Roskilde, Denmark*

(* Corresponding author: akpr@dtu.dk)

**Abstract:** When the model dosimetry system $YPO_4$: $Sm^{3+}$, $Ce^{3+}$ is exposed to X-rays, the charge state of the dopants changes, becoming $Sm^{2+}$ and $Ce^{4+}$ via electron and hole trapping, respectively; the original charge states can be achieved through electron transfer back from $Sm^{2+}$ to $Ce^{4+}$ via optical stimulation. The work presented here adds further details to the energy levels of the metastable $Sm^{2+}$ defect and the electron transfer processes by undertaking measurements of a) $Sm^{2+}$ excitation spectrum through the internal $^5D_0 \rightarrow {}^7F_2$ emission at 7 K, b) relaxation lifetime of $Sm^{2+}$ ($^5D_0$ state) and its temperature dependence to provide insights into thermal quenching, and c) the kinetics of localised recombination from $Sm^{2+}$ to $Ce^{4+}$ on nanoseconds to seconds time scales using sub-band-edge excitation.

**Keywords:** radio-photoluminescence, low temperature spectroscopy, localised recombination, excited-state tunnelling, thermal quenching, $Sm^{2+}$ and $Ce^{3+}$ relaxation lifetime

## 1. Introduction

Doping wide band-gap materials with rare earth ions introduces defect levels within the bandgap which makes them useful in many applications, such as charge storage phosphors for use in luminescence dosimetry (Chakrabarti et al, 1989, Meijerink et al, 1991), display phosphors and optical memory (Thiel et al, 2002, Ding et. al., 2016), and persistent luminescent materials (Matsuzawa et. al., 1996, Hölsa et al., 2001). The extensive knowledge accumulated over the last

four to five decades in identifying the behaviour and energy levels of lanthanide dopants within the band gap of a host material gives us a clear idea about whether they will act as an electron or a hole trap on exposure to ionizing radiation (for summary, see Dorenbos et al., 2003, 2011). In this respect, $YPO_4$ co-doped with $Sm^{3+}$ and $Ce^{3+}$ ions shows excellent promise as a model system for fundamental studies: on irradiation with X–rays, these defects form the metastable states $Sm^{2+}$ and $Ce^{4+}$ whose energy levels can be precisely characterised for controlled charge transfer (Dorenbos et al., 2003, Poolton et al, 2012).

Previous work to understand the luminescence charge transfer properties of $YPO_4$:$Ce^{3+}$, $Sm^{3+}$ have used synchrotron radiation (4-20 eV) and both optical and thermoluminescence spectroscopy (Pieterson et al., 2001; Poolton et al, 2010, 2012; Dorenbos et al., 2011; Mandowski and Bos, 2010; Bos et al., 2010). These studies have also allowed determination of the electron and hole trap energies within the band-gap. However, understanding the precise nature of energy transfer from $Sm^{2+}$ to $Ce^{4+}$ processes requires detailed information concerning the excited state energy levels of the metastable $Sm^{2+}$ defect, and this is still very much work-in-progress. The first indications of the defect's excited state energy levels came from the optically stimulated luminescence (OSL) excitation spectra measured via the $Ce^{3+}$ emission (Bos et al, 2010). As this involves excited-state tunnelling from $Sm^{2+}$ to $Ce^{4+}$, the transitions were significantly broadened due to interference with 4f 5d (SmA, SmB) bands (which are the most effective conduit for the tunnelling), and only limited spectroscopic information was obtainable. By using a low flux, 1.92 eV laser stimulation at 10 K, Poolton et al (2012) were able to exclusively probe isolated $Sm^{2+}$ emission 4f-4f transition, and thereby determine the ground state energy levels in more detail. In the same study a 2.33 eV laser probe for the emission at 10 K confirmed the simultaneous presence of both stable $Sm^{3+}$ ions and metastable $Sm^{2+}$ ions in the $YPO_4$ host.

Regarding charge transfer, the OSL in $YPO_4$: Sm, Ce has previously been studied using the 2.79 eV excitation which photo-ionises the $Sm^{2+}$ followed by recombination via the conduction band (delocalised charge transfer) at the $Ce^{4+}$ (Poolton et al., 2010). In contrast, thermal decay (TL) has shown a tunnelling emission corresponding to a continuum of localised recombination probabilities, superimposed on the TL peaks produced by delocalised recombination (Dobrowolska et al., 2014). Detailed understanding of the tunnelling kinetics is tedious using the TL signal because of a continuum of temperature dependent excitation probabilities and an overlap between localised and

delocalised processes. This problem can be avoided using an energy specific, sub-bandgap excitation leading to a direct charge transfer from $Sm^{2+}$ to $Ce^{4+}$.

The missing details of the $YPO_4$:$Ce^{3+}$, $Sm^{3+}$ model system are: knowledge about the exact energy levels of the excited state of metastable $Sm^{2+}$, and the relaxation rates from the excited-to-ground states of the ion. Furthermore, the charge transfers kinetics using $Sm^{2+}$ excited state tunnelling is not understood at the moment; there is a general need for such information on model systems, as it is important for testing and refining our theoretical understanding of stimulated localised recombination emission (e.g. see Jain et al. 2012, 2015).

In this article, we move towards a more complete picture of the $YPO_4$: Ce, Sm model system by measuring for the first time the detailed excitation spectra of metastable $Sm^{2+}$ at 7 K via the $Sm^{2+}$ emission itself; this allows us to determine the precise location of the ion's excited states. We also measure the temperature dependent relaxation lifetime and dose-dependency of this internal $Sm^{2+}$ emission (Stokes shifted OSL or radio-photoluminescence), without relying on any charge transfer to $Ce^{4+}$. Finally, we study the optically stimulated tunnelling recombination from the excited states of $Sm^{2+}$ to the $Ce^{4+}$. The method of isolating the luminescence processes of individual metastable defects (rather than relying on the charge transfer between defects) is an important outcome of this work which can be applied to the other lanthanide co-dopants, as well as to complex natural materials, such as feldspars.

## 2. Instrumentation and sample details

The yttrium phosphate sample used in this study was co-doped with 0.5% cerium and 0.5% samarium, and prepared by solid state reaction (for details, see Bos et al, 2008). All measurements were made using the Risø station for CryOgenic LUminescence Research (COLUR) at DTU Nutech. This system consists of a Horiba Fluorolog-3 spectrofluorometer, upgraded to include a temperature controlled (7-300 K) closed-loop cryostat, an X-ray irradiation facility (40 kV, 100 µA copper anode with 3 ms action X-ray shutter), and multiple ports for laser excitation and photo-detection, for use in a number of dual-probe type experiments. The sample is in vacuum, attached directly to the cryostat cold finger.

Luminescence excitation spectra were measured with a 450 W Xenon CW lamp and detected with a photomultiplier tube (PMT; S1 response). A series of appropriate long-pass filters were placed between the sample and the emission monochromator to remove second order excitation light.

Time resolved luminescence measurements were measured using time-correlated single photon counting (TCSPC), with a 657 nm (~ 1.89 eV) laser diode as the source. The laser has a maximum power of 40 mW, and works in either CW mode, or can be modulated up to 155 MHz with rise/fall times of < 3 ns, with a minimum pulse width ~ 50 ns. Dose-dependent OSL curves were obtained with the laser in CW mode and directly recorded using a PMT (with U340 filters), external to the Fluorolog monochromators; this exclusively samples the $Ce^{3+}$ emission.

## 3. Results and Discussion

### 3.1 Low temperature luminescence properties of $Sm^{2+}$

X-irradiation of $YPO_4$: Ce, Sm **(**9.2 eV bandgap) leads to the formation of free electrons and holes. The original charge states of the dopants ($Sm^{3+}$, $Ce^{3+}$) change to metastable state ($Sm^{2+}$, $Ce^{4+}$). On capturing the electrons and holes they return to their original ($Sm^{3+}$, $Ce^{3+}$) configuration after several days via non-radiative ground-state tunnelling, or via external stimulation by heat or light resulting in TL and OSL, respectively. Fig. 1(a) shows the laser excited $Sm^{2+}$ emission spectra at 7 K for different X-ray irradiation durations. The emission arises exclusively from the internal 4f ($^5D_0 \rightarrow {}^7F_{2,3,4}$) transitions at 1.70, 1.64 and 1.54 eV, respectively, all of which increase in intensity with dose. The dose-dependent change in the PL intensity confirms that we are directly probing the metastable $Sm^{2+}$; such signal in dosimetry is commonly named as radio-photoluminescence (Schulman et.al., 1951). Only some $Sm^{3+}$ are converted to $Sm^{2+}$ and the inset to Fig. 1(a) shows the $^4G_{5/2} \rightarrow {}^6H_{5/2\ ,7/2,\ 9/2,\ 11/2}$ transitions of $Sm^{3+}$, excited in a non-dosed sample under 3.06 eV laser excitation; the separate spectral emission features of $Sm^{2+}$ and $Sm^{3+}$ are clearly distinguished. These results are in good agreement with those of Poolton et al. (2012) confirming the reliability of our measurements.

The excitation spectrum of $Sm^{2+}$ was recorded at 7 K after 3 hours of X-ray irradiation with the detection fixed at 1.70 eV (the $^5D_0 \rightarrow {}^7F_2$ transition) and the excitation energy varying from 1.75 to 2.05 eV (Fig.1b). As $Sm^{2+}$ has a trap depth of 2.3 eV (Bos et al., 2010; Poolton et al., 2010) excitation in the energy range 1.75 - 2.1 eV has insufficient energy to evict charge from the centre

via the conduction band. The observed peaks, therefore, represent the internal transitions within $Sm^{2+}$, an interpretation further strengthened by the fact that the signal does not decay with time (steady state). The clearly resolved peaks in the present excitation spectrum contrast with those in previous work where the transitions were observed via $Ce^{3+}$ emission by excited state tunnelling (Dorenbos et al., 2011, Bos et al, 2010, Poolton et al, 2010, 2012); this charge transfer process in the earlier work led to extensive broadening of the transitions, making most of the features almost indistinguishable. The resolution of the spectral features obtained here allow for the first time a clear identification of the excited levels of $Sm^{2+}$ in $YPO_4$ host. These excitation peaks arise from internal 4f-4f transitions of $Sm^{2+}$ and, in combination with the previous work regarding analysing the emission lines (Poolton et al, 2012), we tentatively assign $^7F_0 \rightarrow {}^5D_{0,1,2,3}$ at 1.837, 1.879, 1.898 and 1.977 eV respectively, and $^7F_1 \rightarrow {}^5D_0$ at 1.785 eV. Low intensity phonon replicas (~20 meV) associated with each electronic transition are also observed.

The time resolved luminescence of the main $Sm^{2+}$ peak emission excited using the 1.89 eV laser at 7 K, is shown in Fig.1(c); the inset shows the relevant excitation and emission energy levels. The data, when fitted with a single exponential function, yield lifetimes of 751 ± 16, 729 ± 11 and 704 ± 10 ns for the emission peaks at 1.54, 1.64 and 1.70 eV respectively (corresponding to $^5D_0 \rightarrow {}^7F_{4,3,2}$). These lifetime estimates are consistent within 2σ uncertainty.

### 3.2 Temperature dependent luminescence properties of $Sm^{2+}$

The temperature dependence of the $Sm^{2+}$ PL emission excited by the 1.89 eV laser is shown in Fig. 2(a). This shows that the peaks at 1.70 eV and 1.64 eV ($^5D_0 \rightarrow {}^7F_{2,3}$) are broadened as the temperature is increased in the range of 100-300 K, and the peaks become rapidly quenched at temperatures higher than 130 K. This thermal quenching behaviour of $Sm^{2+}$ has been reported before by Poolton et al. 2012; our data mimics the trend reported by these authors.

Thermal enhancement and thermal quenching of a signal can occur due to interplay of many different mechanisms (see for e.g. Pal et al., 2013). In comparison to PL intensity, the lifetime is a more robust parameter to understand thermal quenching due to a non-radiative pathway. Therefore, in order to accurately define the kinetics of thermal quenching in our signal we examined the lifetime dependence of $Sm^{2+}$ on temperature.

Fig. 2(b) shows the luminescence decay of the $Sm^{2+}$ emission at 1.7 eV ($^5D_0 \rightarrow {}^7F_2$) at different temperatures, analysed in each case with single exponential function (after background subtraction).

The average lifetime of the $Sm^{2+}$ emission at 1.7 eV ($^5D_0 \rightarrow {}^7F_2$) in the temperature range 10-140 K yields 706 ± 5 ns, whereas at higher temperature the lifetime decreases very rapidly, being ~ 98 ± 1 ns at 220 K. Fig. 2(c) shows the temperature dependence of the integrated PL intensity for emission peaks between 1.69-1.72 eV (denoted as "1.7 eV") and the temperature dependence of the lifetime for the 1.7 eV emission peak. We note that the 1.625-1.65 eV (denoted as "1.64 eV") emission showed the same trend as 1.7 eV peak (not shown here for clarity).

The lifetime data show an excellent reproducibility (Fig. 2(c)). The lifetime and the PL data show a broadly similar trend with temperature, suggesting that Mott-Seitz mechanism can explain the overall thermal quenching of the $Sm^{2+}$ photoluminescence in the $YPO_4$: Ce, Sm system; in this mechanism, the increased probability of non-radiative relaxation pathway at higher temperature leads to a simultaneous reduction in signal intensity and a lower lifetime (e.g., Ueda et. al., 2015, Pal et al. 2013, Calderon et al, 1990, Pagonis et al., 2010). We note that tunnelling loss through the SmA and SmB bands becomes detectable above 200 K (Fig. 5 of Poolton et al., 2012), and is, therefore, not likely to be responsible for the decreasing trend observed in our data up to at least 200 K. A slight deviation in the PL and lifetime data may originate due to thermal partitioning of electrons in the ground states ($^7F$ multiplet) of the $Sm^{2+}$, which will vary with temperature and likely affect the PL intensity; but this effect will not alter the excited state lifetime.

Based on the Mott-Seitz mechanism, the temperature dependence of lifetime can be described by the following function (Pal et al. 2013; Calderon et al, 1990):

$$\frac{1}{\tau(T)} = \frac{1}{\tau_r} + \frac{1}{\tau_{nr}} exp\left(\frac{-\Delta E}{kT}\right) \qquad (1)$$

Where $\tau(T)$ is the measured temperature dependent lifetime, $1/\tau_r$ is probability of radiative transition, where $\tau_r$ corresponds to the measured lifetime before the onset of thermal quenching, $1/\tau_{nr}$ is the frequency factor for the non-radiative transition probability, $\Delta E$ is the threshold energy for non-radiative transition and $k$ is Boltzmann's constant. The fitting of equation (1) to the lifetime data (Fig. 2(c)) yielded a quenching energy of 0.20 ± 0.005 eV, $\tau_r$ = 706 ± 5 ns, and $1/\tau_{nr}$ = 5.4 ± 1.8 x $10^{11}$ $s^{-1}$.

Similarly, the reduction in the PL intensity with temperature can be analysed using the thermal quenching equation, which can be derived from Eq (1) (Chitambo et al., 2007).

$$I(T) = \frac{I(0)}{1+Cexp(-\Delta E/kT)} \qquad (2)$$

Here *I(T)* represents the integrated PL intensity at temperature *T* (K), I(0) is the intensity at absolute zero temperature; $\Delta E$ (eV) is the thermal quenching energy and *k* (eV. $K^{-1}$) is the Boltzmann's constant, and *C* is a constant equal to the ratio $\tau_r/\tau_{nr}$ (Calderon et al, 1990; Pagonis et al. 2010, Chithambo et al., 2007). The fit for Eq. (2) to the PL intensity data is shown as a dashed curve in Fig. 2(c). This fit gives slightly different values than those derived from the lifetime data ($\Delta E$= 0.14 ± 0.01 eV; C= 6.1 ± 4.7x$10^3$); note that the value of C derived from the best fit to the lifetime data is 3.8x$10^5$. Because of the reasons discussed before, i.e. that the affect of the ground state on the PL intensity, we consider the lifetime data to be a more reliable indicator of the thermal quenching kinetics; thus we conclude that the threshold for non-radiative transition for $^5D_0$ state of $Sm^{2+}$ in $YPO_4$ is ~ 0.20 eV.

### 3.3 Optically induced tunnelling luminescence

As mentioned earlier, electrons from excited states of $Sm^{2+}$ (SmA and SmB bands); can transfer via tunnelling to the $Ce^{4+}$ centre, resulting in $Ce^{3+}$ emission; although this mechanism has been used earlier to characterise the $Sm^{2+}$ defect (Bos et al., 2010; Poolton et al., 2012), the kinetics of the optically induced charge transfer process have not been explored before. After irradiating the sample with X-rays, we excited $Sm^{2+}$ with 1.89 eV laser at room temperature and measured the resulting luminescence signal from the $Ce^{3+}$ emission (with U340 filters). Fig. 3(a) shows the OSL emission spectrum resulting from this process. As expected this emission grows with X-ray irradiation time due to increased concentrations of $Sm^{2+}$ and $Ce^{4+}$. The characteristic 5d-4f emission doublet of $Ce^{3+}$ is clearly observed at 3.47 eV and 3.73 eV; this arises from the $5d_1 \rightarrow {}^2F_{7/2,\ 5/2}$ transitions (Laroche et al, 2001).

To understand the dynamics of the optically induced tunnelling process, we made Time-Resolved OSL (TR-OSL) measurements using 1.89 eV laser excitation for both the emissions, i.e. 3.47 eV and 3.73 eV. Fig. 3(b) shows the obtained TR-OSL data which show an exponential decay. These data were fitted with a single exponential function, yielding lifetimes 19.4 ± 0.1 ns and 19.2 ± 0.6 ns for 3.47 eV and 3.73 eV emission peaks, respectively. These lifetimes correspond well with the published lifetime of $Ce^{3+}$ excited state (Laroche et al., 2001) which was 23 ns. Interestingly, the predicted $^5D_0$ excited state lifetime of $Sm^{2+}$ at room temperature is about 7 ns based on the

parameters derived from Equation (1), implying that the $^5D_0$ could potentially be feeding to the tunnelling active states (SmA and SmB bands) and thereby $Ce^{4+}$, while the $Ce^{3+}$ excited state relaxation is ongoing; this process could give rise to an initial non-exponentially (peak shape) in the TR-OSL. However, based on our TR-OSL data, it can be inferred that both the $^5D_0$ and the tunnelling active states in the $Sm^{2+}$ must empty very rapidly (at least an order of magnitude faster than the $Ce^{3+}$ relaxation rate) at room temperature so as to give clean single exponential decay representative of $Ce^{3+}$. Thus at room temperature there must be much faster emptying of the $^5D_0$ state (possibly to the tunnelling bands) than that predicted by thermal quenching model, and an insignificant retrapping from the tunnelling active states to the $^5D_0$ state.

Since the excitation with 1.89 eV is sub-conduction band, the only mechanism of charge transfer is tunnelling from $Sm^{2+}$ excited state to $Ce^{4+}$. Understanding the excited state tunnelling process is of interest in order to understand the behaviour of both artificial and natural dosimeters (e.g. see Jain et al., 2012). However, this understanding is usually hampered by complexity of the materials of interest. For example, decades of research has been devoted to tackling the anomalous fading problem in feldspars, which arises due to tunnelling loss from the dosimetric trap (see Jain and Ankjærgaard, 2011 for a comprehensive discussion). Our model $YPO_4$: Ce, Sm gives us an opportunity to isolate the excited state tunnelling process and use it to test our theoretical understanding of tunnelling in randomly distributed defects. With this objective we measured the CW-OSL using the 1.89 eV laser excitation after different X-ray irradiation durations. Fig. 4(a) shows the CW-OSL decay curves recorded using a separate PMT with U340 filters; the corresponding emission spectra are plotted in Fig. 3(a).

The truncated-distribution tunnelling OSL model of Jain et al (2015) predicts that the shape of the OSL decay curve should depend both on the hole density (e.g. due to increasing dose), and on the truncation of the nearest neighbour distribution (e.g. due to prior heating or ground state tunnelling). We apply their model equation to our data in Fig. 4 (a) obtained after different X-ray irradiation times:

$$OSL \propto -\frac{dn}{dt} = 3n_0\rho' z\,(t')^{-1}[\ln(t'b) - \xi]^2 \exp\{-\rho'[\ln(t'b) - \xi]^3\} \qquad (3)$$

Here $n$ is the instantaneous, $n_0$ the initial trapped electron concentration, $\rho'$ is the number density of the trapped holes, $b$ [$s^{-1}$] is the attempt to tunnel frequency, $t'$ is a variable, which is a linear function of time ($\tau_0$ + zt), $\xi = \ln(s/p)$, where s is frequency factor and p is optical excitation probability per unit time. The equation (3) fits well to all the OSL curves in Fig. 4(a) confirming that the excited state tunneling model describes well the observed OSL signal produced by localized recombination. Two fitting parameters that deserve closer scrutiny here are the dimensionless hole density $\rho'$, which should increase with dose, and the truncation parameter $\tau_0$ which should increase with irradiation time because of ground state tunneling. Both these parameters are plotted in Fig. 4(b); their trend with X-ray irradiation time (or dose) confirms the model predictions (Equation 3).

## 4. Conclusion:

Using low temperatures and sub-conduction-band excitation, new details of the metastable $Sm^{2+}$ defect in co-doped, irradiated $YPO_4$: Ce, Sm have been measured, including details of the excited states, measurement of the internal 4f-4f time decay constants, and dynamics of the optically induced excited-state tunnelling pathways for electron recombination at $Ce^{4+}$. The methods are ideal for exploring metastable states in other lanthanide co-doped wide band-gap materials, and for understanding charge recombination processes in complex natural dosimeters such as feldspars.

## 5. Acknowledgment

Prof. A. J. J. Bos is thanked for providing $YPO_4$: Ce, Sm sample and Dr. N. R. J. Poolton is thanked for participation during the various stages of this study. Dr. Torben Lapp is thanked for his support in the commissioning of low temperature facility.

## References


Bos, A. J. J., Dorenbos, P., Bessière, A, Viana, B., (2008) Lanthanide energy levels in $YPO_4$. Radiation Measurements 43, 222 – 226

Bos, A. J. J., Poolton, N. R. J., Wallinga, J., Bessière, A., Dorenbos, P. (2010). Energy levels in $YPO_4:Ce^{3+}$, $Sm^{3+}$ studied by thermally and optically stimulated luminescence. Radiat. Meas. 45, 343-346.

Calderon, T, Millan, Jaquet, F., Sole, G., J. (1990) Optical properties of $Sm^{2+}$ and $Eu^{2+}$ in natural fluorite crystals. Nucl. Tracks Radiat. Meas.,17, 557-561

Chakrabarti, K., Mathur, V.K., Thomas, L.A., Abbundi, R.J., (1989). Charge trapping and mechanism of stimulated luminescence in CaS: Ce; Eu. J. Appl. Phys. 65, 2021–2023.

Chithambo, M.L., 2007. The analysis of time-resolved optically stimulated luminescence. II: Computer Simulations and Experimental Results. J. Phys. D.: Appl. Phys. 40, 1880-1889.

Dorenbos, P., (2003) Systematic behaviour in trivalent lanthanide charge transfer energies J. Phys.: Condens. Matter 15, 8417–843

Dorenbos, P., Bos, A. J. J., Poolton, N. R. J. (2011) Electron transfer processes in double lanthanide activated $YPO_4$, Optical Materials 33, 1019–1023

Ding, D., Pereira, L. M. C., Bauters, J. F., Heck, M.J. R., Welker, G., Vantomme, A., Bowers, J. E., Dood, M.J. A., Bouwmeester, D.(2016) Multidimensional Purcell effect in an ytterbium-doped ring resonator. Nature Photonics **10**, 385–388

Dobrowolska, A., Bos, A. J. J., Dorenbos, P. (2014) Electron tunnelling phenomena in YPO4: Ce, Ln (Ln= Er, Ho, Nd, Dy). Journal of Physics D: Applied Physics 47, 33

Hölsa, J., Jungner, H., Lastusaari, M., Niittykoski, J., (2001). Persistent luminescence of $Eu^{2+}$ doped alkaline earth aluminates, $MAl_2O_4$: $Eu^{2+}$. J. Alloys Compd. 323, 326–330.

Jain, M., Sohbati, R., Guralnik, B., Murray, A., Kook, M., Lapp, T., Prasad, A.K., Thomsen, K.J., Buylaert, P., (2015). Kinetics of infrared stimulated luminescence from feldspars. Radiat. Meas. 81, 16-22.

Jain, M., and Ankjærgaard, C., (2011). Towards a non-fading signal in feldspar: Insight into charge transport and tunnelling from time-resolved optically stimulated luminescence. Radiation Measurements, 46, 292–309.

Jain, M., Guralnik, B., Andersen, M. T. (2012) Stimulated luminescence emission from localized recombination in randomly distributed defects. Journal of physics: Condensed matter 24, 385402.

Laroche, M., Girard, S., Margerie, J. Moncorge, J., Bettinelli, M., Cavalli,E.,(2001) Experimental and theoretical investigation of the $4f^n \leftrightarrow 4f^{n-1}5d$ transitions in $YPO_4:Pr^{3+}$ and $YPO_4:Pr^{3+}, Ce^{3+}$. J. Phys.: Condens. Matter, 13, 765–776

Meijerink, A., Schipper, W.J., Blasse, G., (1991). Photostimulated luminescence and thermally stimulated luminescence of $Y_2SiO_5 : Ce^{3+}, Sm^{3+}$. J. Phys. D: Appl. Phys. 24, 997–1002

Mahbubulalam, A. S. M, and Bartolo, B. Di, (1967). Deexcitation and lifetime of $^5D_0$ state in optically pumped $SrF_2:Sm^{2+}$. Physics Letters, 25A.

Mandowski, A., Bos, A. J. J. (2011) Explanation of anomalous heating rate dependence of thermoluminescence in $YPO_4:Ce^{3+}$, $Sm^{3+}$ based on the semi-localized transition (SLT) model Radiation Measurements 46 1376-1379

Matsuzawa, T., Aoki, Y., Takeuchi, N., Murayama, Y., (1996). New long phosphorescence phosphor with high brightness, $SrAl_2O_4: Eu^{2+}, Dy^{3+}$. J. Electrochem. Soc. 143, 2670–2673.

Pal, P., Penhouët, T., D'Anna ,V., Hagemann, H.(2013) Effect of temperature and pressure on emission lifetime of $Sm^{2+}$ ion doped in MFX (M=Sr, Ba; X=Br, I) crystals. J. Lumin., 142, 66–74

Pieterson, L. V., Reid, M. F., Burdick, G. W., and Meijerink , A.(2001). $4f^n \leftrightarrow 4f^{n-1}5d$ transitions of the light lanthanides: Experiment and theory. Phys. Rev. B 65, 045113

Poolton, N. R. J., Bos, A. J. J., Dorenbos, P. (2012). Luminescence emission from metastable $Sm^{2+}$ defects in $YPO_4$: Ce, Sm.J. Phys.: Condens. Matter 24,225502

Poolton, N. R. J., Bos, A. J. J., Jones, G.O., Dorenbos, P (2010). Probing electron transfer processes in YPO4: Ce, Sm by combined synchrotron–laser excitation spectroscopy. J. Phys.: Condens. Matter 22, 185403

Pagonis, V., Ankjærgaard, C., Murray, A., Jain, M., Chen, R., Lawless, J., Greilich, S. (2010). Modelling the thermal quenching mechanism in quartz based on time-resolved optically stimulated luminescence. Journal of Luminescence, 130(5), 902-909

Schulman, J.H., Ginther, R.J., Klick, C.C., Alger, R.S., Levy, R.A. (1951). Dosimetry of X-rays and gamma-rays by radiophotoluminescence. J. Appl. Phys. 22, 1479-1487.

Thiel, C.W., Sun, Y., Cone, R.L., (2002). Progress in relating rare-earth ion 4f and 5d energy levels to host bands in optical materials for hole burning, quantum information and phosphors. J. Mod. Opt. 49, 2399–2411.

Ueda, J., Dorenbos, P., Bos, A. J. J., Meijerink, A., Tanabe, S. (2015) Insight into the Thermal Quenching Mechanism for $Y_3Al_5O_{12}:Ce^{3+}$ through Thermoluminescence Excitation Spectroscopy. J. Phys. Chem. C, 119, 25003−25008

**Figure Captions**

**Figure 1**

(a) Emission features of metastable $Sm^{2+}$ in $YPO_4$: Ce, Sm, under 1.89 eV stimulation after 30, 45 and 60 minutes of X-ray irradiation (black, blue and red curves, respectively). The inset shows emission corresponding to $Sm^{3+}$ in un-irradiated material, using 3.06 eV laser.
(b) Excitation spectrum of $Sm^{2+}$ in $YPO_4$: Ce, Sm after 3 hours of X-ray irradiation, recorded for emission fixed at 1.7 eV. (c) Time-resolved measurement of $Sm^{2+}$ emissions under 1.89 eV laser stimulation, fitted with a single exponential function. The inset shows the relevant energy levels. All measurements are made at 7 K.

**Figure 2**

Temperature dependence of the $Sm^{2+}$ emission under 1.89 eV laser excitation, after 3 hours of X-ray irradiation: (a) emission spectra, (b) Time-resolved measurement of $^5D_0 \rightarrow {}^7F_2$, transitions fitted with an exponential function, and (c) lifetime and integral PL intensity as a function of measurement temperature; the data are fitted with equation (1) and (2), respectively (see text).

**Figure 3**

Characteristics of optically stimulated luminescence emission arising from excited state tunnelling from metastable $Sm^{2+}$ to $Ce^{4+}$ states. The signals are detected from $Ce^{3+}$ emission produced by electron recombination at the $Ce^{4+}$center. The data are recorded at room temperature under 1.89 eV laser excitation. (a) OSL emission spectra produced after different X-ray irradiation durations (or dose), and (b) Time-resolved OSL emissions (3.47 and 3.73 eV) fitted with a single exponential function.

**Figure 4**

(a) OSL decay curves produced after different X-ray irradiation durations (or dose); these data are fitted with the truncated distribution tunnelling model (Equation 3), (b) Dimensionless hole density ( $\rho'$) and the truncation parameter $\tau_0$ derived from fitting of OSL decay curves in Fig. 4(a), plotted as a function of X-ray irradiation duration (see text).

Figure 1

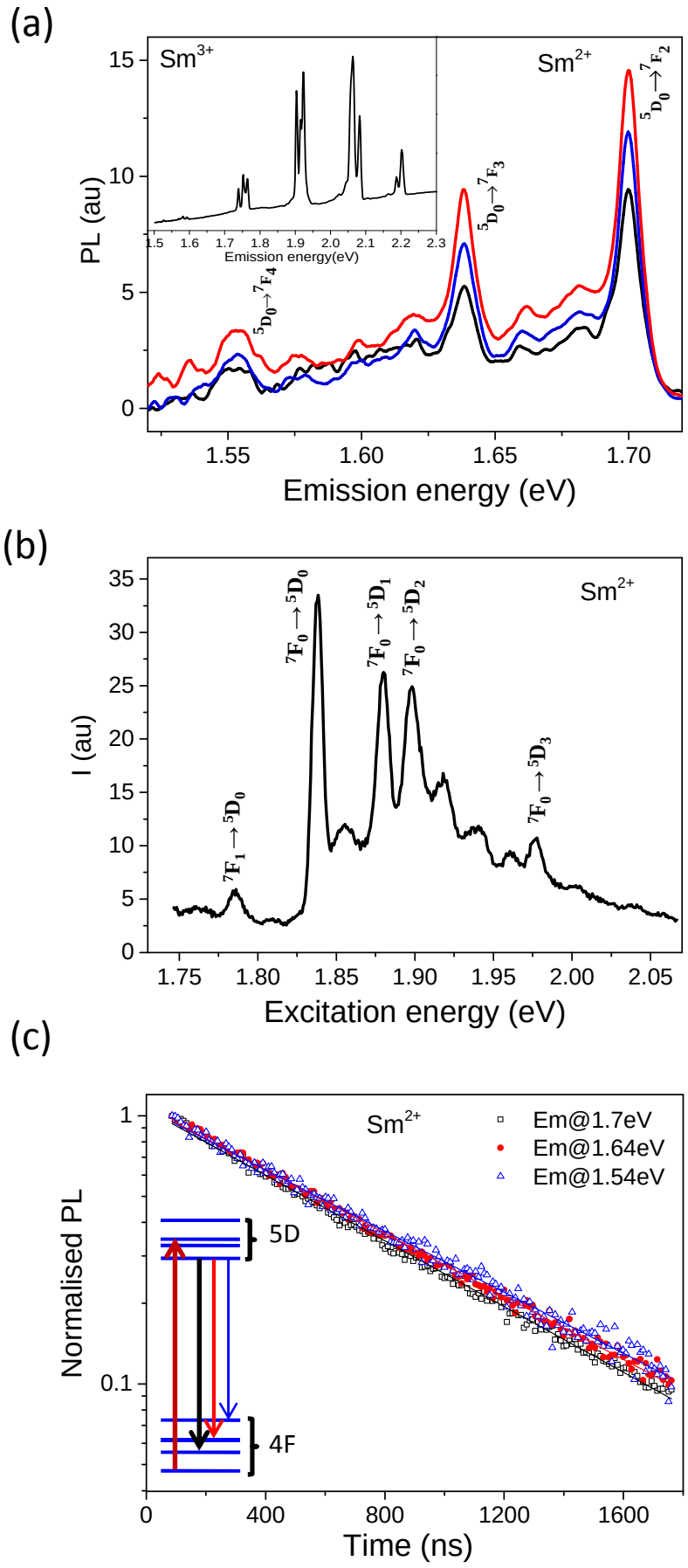
(a)
Sm3+
Sm2+
PL (au)
Emission energy (eV)
5D0→7F4
5D0→7F3
5D0→7F2
(b)
Sm2+
I (au)
Excitation energy (eV)
7F1→5D0
7F0→5D0
7F0→5D1
7F0→5D2
7F0→5D3
(c)
Sm2+
Em@1.7eV
Em@1.64eV
Em@1.54eV
Normalised PL
Time (ns)
5D
4F

Figure 2

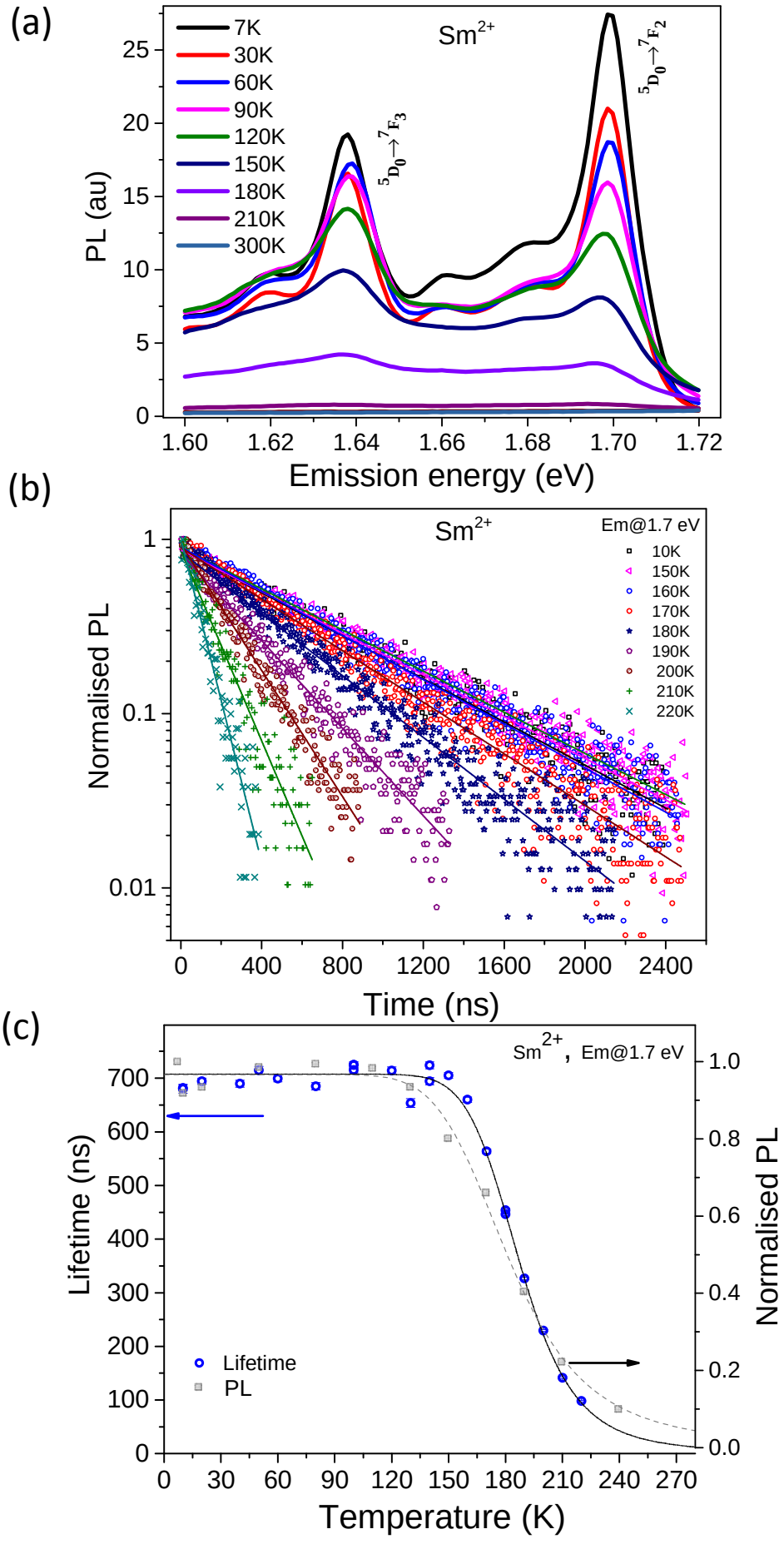
(a)
7K
30K
60K
90K
120K
150K
180K
210K
300K
Sm2+
5D0→7F3
5D0→7F2
PL (au)
Emission energy (eV)
(b)
Sm2+
Em@1.7 eV
10K
150K
160K
170K
180K
190K
200K
210K
220K
Normalised PL
Time (ns)
(c)
Sm2+, Em@1.7 eV
Lifetime
PL
Lifetime (ns)
Normalised PL
Temperature (K)

Figure 3

(a)

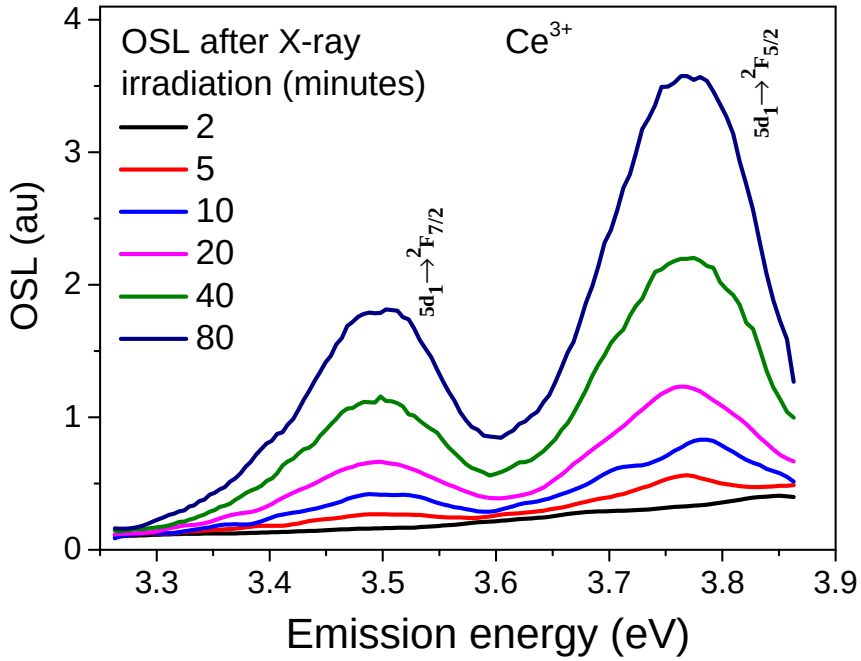
OSL after X-ray
irradiation (minutes)
2
5
10
20
40
80
Ce3+
5d1→2F7/2
5d1→2F5/2
OSL (au)
Emission energy (eV)
0
1
2
3
4
3.3
3.4
3.5
3.6
3.7
3.8
3.9

(b)

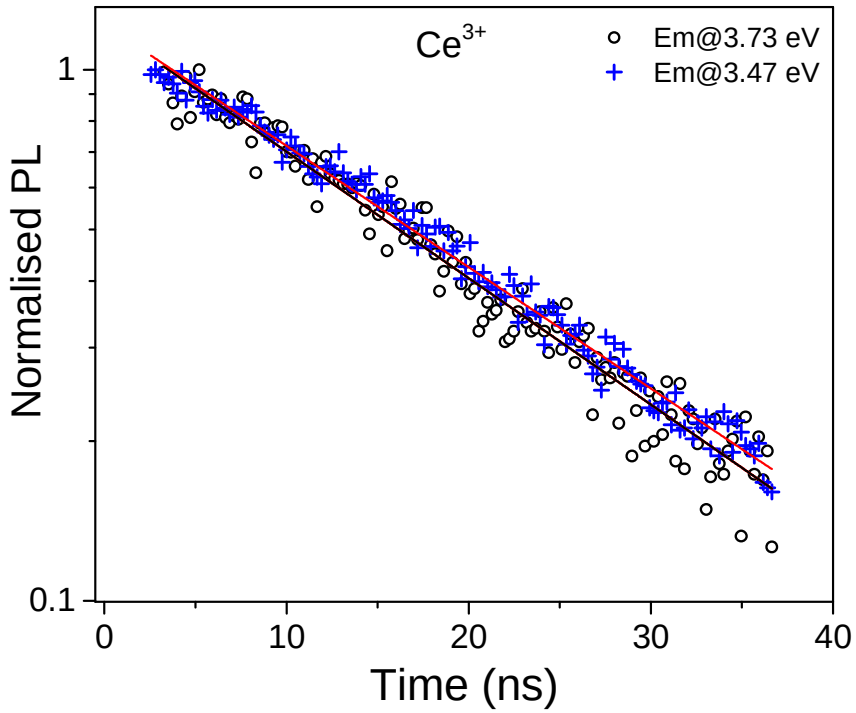
Ce3+
Em@3.73 eV
Em@3.47 eV
Normalised PL
Time (ns)
1
0.1
0
10
20
30
40

Figure 4

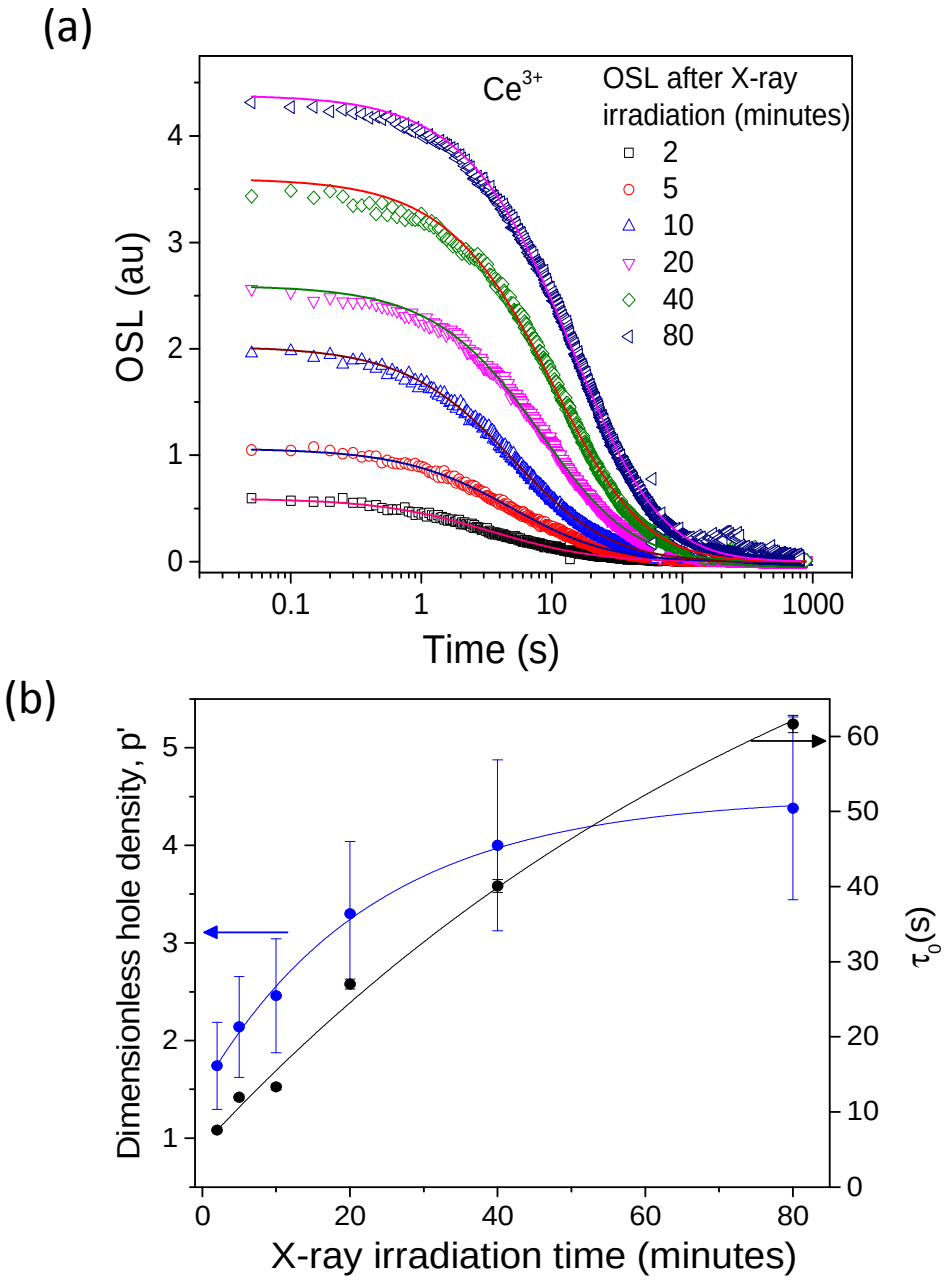
(a)
Ce3+
OSL after X-ray irradiation (minutes)
2
5
10
20
40
80
OSL (au)
Time (s)
0.1
1
10
100
1000
(b)
Dimensionless hole density, p'
τ0(s)
X-ray irradiation time (minutes)
0
20
40
60
80

# Highlights: Probing Metastable $Sm^{2+}$ and Optically Stimulated Tunnelling Emission in $YPO_4$: Sm, Ce

- The detailed excitation spectrum of metastable $Sm^{2+}$ at 7 K through its internal emission.
- Thermal quenching and temperature dependent relaxation lifetime of $Sm^{2+}$.
- Kinetics of optically stimulated tunnelling recombination.